ORIGINAL PAPER

physica
pssa
status solidi a
www.pss-a.com

Spectral Characteristics and Spatial Distribution of Thermal Donors in n-Type Czochralski-Silicon Wafers

Espen Olsen,* Malin I. Helander, Torbjørn Mehl, and Ingunn Burud

In monocrystalline silicon rich in oxygen, thermal donors are formed at temperatures around 450 °C. These are widely accepted to be electrically active oxygen clusters acting as double donors to the conduction band. Exposure to higher temperatures (650 °C) reportedly eliminates them. Herein, a systematic study of the spatial distribution of thermal donor formation and elimination by heat treatment at 450 and 650 °C in commercial n-type Czochralski-silicon wafers with high and low content of interstitial oxygen atoms are reported. Hyperspectral imaging techniques with spectral and spatial resolution are used. Thermal donors form at 450 °C in a ring-like pattern, significantly enhanced in oxygen-rich material. The results indicate the formation of at least six different donor clusters, leading to a strong, characteristic spectral response upon photoexcitation. The emission related to direct band-to-band recombination (1.100 eV) become systematically stronger upon heat treatment at 450 °C. Subsequent treatment at 650 °C rearrange the spectral response into a single, homogenously distributed, broadband emission with peak energy of 0.767 eV. The emission related to band-to-band recombination is significantly reduced. A previously studied emission at 0.807 eV (D1) commonly related to impurities is found, providing evidence that this signal is related to the combination of defects and oxygen.

1. Introduction

The Czochralski (Cz) technique is commonly used in the growth of monocrystalline silicon ingots. In this process, the defects can get introduced into the material. These can be both structural point defects, such as interstitials and vacancies, and impurities as a result of contamination. The biggest challenge in the Cz-silicon production lays in reducing oxygen- and carbon-related defects. Both are introduced into the material from multiple sources in the production process. The quartz crucible and carbon furnace components are the main sources for oxygen and carbon constituting the main impurities. Interstitial oxygen (O_i) and

Prof. E. Olsen, M. I. Helander, Dr. T. Mehl, Prof. I. Burud
Faculty of Science and Technology
Norwegian University of Life Sciences (NMBU)
Universitetstunet 3, 1432 Ås, Norway
E-mail: espen.olsen@nmbu.no

The ORCID identification number(s) for the author(s) of this article can be found under https://doi.org/10.1002/pssa.201900884.

substitutional carbon (C_s) are in general not considered to be electrically active and so are not supposed to lead to enhanced recombination of charge carriers. However, minor amounts of other contaminants such as iron are also introduced from the crucible, feedstock, and furnace construction materials. These are frequently electrically active introducing states in the bandgap of silicon acting as sites for recombination. Thermal donor (TD) is widely accepted to be formed of smaller clusters of oxygen in the silicon structure and is commonly found in oxygen-rich material.[1] They are known for affecting the electrical properties of the material leading to higher electrical conductivity and, to a certain extent, recombination of photogenerated charge carriers. The defect is formed in material that is exposed to temperatures around 450 °C for a prolonged time, as at these temperatures the interstitial oxygen atoms diffuse in the silicon structure and form electrically active clusters.[1,2] Different TDs are reported to introduce donor states placed at different energy levels within the bandgap of silicon.[3] It has further been suggested that the various types of TD differ in cluster size, and that larger clusters form with a long annealing time at 450 °C.[4,5] Photoluminescence (PL) studies have shown that these energy states exist both at a deep and a shallow level in the bandgap.[3] PL emissions that occur due to traps inside the bandgap are categorized as defect-related luminescence (DRL). Several deep-level DRL emissions have been connected to oxygen, such as 0.925 eV, referred to as the H-line and 0.767 eV (P-line), where the latter have been linked to TDs.[6] The structure of the TD clusters has been extensively investigated but is yet to be fully understood.

The first reports of TDs were published as early as 1956 by Fuller and Logan who discovered that Cz silicon exposed to temperatures in the range of 400–500 °C exhibited a significant increase in electrical conductivity due to increased donor concentration.[1] When exposed to long annealing time in the temperature range of 320–500 °C, the donor concentration eventually reached a maximum, and with continued heating a slow decrease started before reaching what is viewed as an equilibrium state. The required time to reach maximum depended on temperature and ingot position of the sample. When the samples were exposed to thermal anneal at temperatures around 600 °C and above, a rapid decrease in donor concentration was noted, ending up with preanneal donor concentrations.

The results made by Fuller and Logan was followed by Kaiser et al. who established the presence of interstitial oxygen (O_i) in silicon.[2] Kaiser et al. found that the initial rate of the donor concentration was proportional to the fourth power of $[O_i]$ and at the donor maximum it was proportional to the third power of $[O_i]$. This work was the first to draw the link between TD and O_i. Since then extensive experimental work has confirmed that interstitial oxygen is involved in the generation of TDs. Consensus at present time is the existence of a distinct set of TD that have a common core, into which oxygen agglomerates.[7] The size of these clusters has been proposed to be affected by the annealing time,[4] and each type of TD will introduce an energy state associated with two electrons in the bandgap and thus act as a double donor.

The decrease in TD after reaching its maximum has been reported in other published work, and the dependency on O_i concentrations and the annealing time needed to reach this maximum is well established.[2,5,8] The generation rate of TD is most probably affected by other point defects in the material as these could interact with the diffusing oxygen. As an example, high concentrations of carbon have shown an inhibiting effect on the formation of TD, proposed to be due to creation of CO complexes.[4] There are conflicting reports on which role self-interstitials or vacancies play in the structure, but a more recent study done by Voronkov et al. showed that higher concentrations of self-interstitials had an enhancing effect on the TD generation rate.[9] Temperatures above 600 °C caused the defect leading to TD to disappear, and these temperatures seem to be enough to cause the O_i atoms to out-diffuse from their specific centers. Only a short-time anneal is needed for donor concentrations to be reduced significantly, as found by Fuller and Logan.[1] In a more recent work by Götz, elimination was performed on samples with both high and low concentrations of TDs.[10] The samples were exposed to temperatures in the range of 520–700 °C, and the results showed that the free electron concentration from donors was reduced in the sample with high initial TD concentration. It, however, increased in the sample with low initial TD concentration. Similar results were obtained when the annealing was performed at higher temperatures, only at a higher rate.

DRL associated with oxygen in Cz-Si has been the topic of a number of studies published primarily in the 1980s. One of the first reports of DRL connected to oxygen was presented by Minaev and Mudryi,[6] where thermally induced defects in silicon-containing oxygen and carbon were investigated. Multiple long-time annealing steps at 450 °C were performed on Cz silicon with both high and low oxygen and carbon contents. The same was done on float-zone (FZ) silicon with high carbon content and very low oxygen content. The presence of numerous DRL emissions in the spectral range of 0.75–1.10 eV was found after annealing steps. Connections between oxygen and DRL peaks at 0.767 eV (P-line) and 0.925 (H-line) was drawn.

Tajima et al. established a connection between interstitial oxygen, TDs, and the emission signal at 0.767 eV.[3] In a wide study of over 60 commercially produced n-type Cz-silicon samples, the P-line persistently appeared when heated at 450 °C for 24 h, and then disappeared at annealing temperatures above 550 °C. Simultaneous measurements of interstitial oxygen and TD concentration were performed. Again, they showed a connection of TD generation and annealing time at 450 °C, and further

presented a dependency between the interstitial oxygen concentration and the intensity of the P-line. They further suggested that the 0.925 eV signal was caused by a CO complex, produced from oxygen and carbon at the same annealing temperatures, as it appeared at strong intensities in samples with carbon concentrations above 4×10^{16} cm^{-3}.

Recently, Kinoshita et al. found that keeping the whole Cz ingot at elevated temperatures (800–1000 °C) during the whole pulling process suppressed the formation of oxygen precipitates in general and TDs in particular.[11] Markevich et al. studied TDs in n-type Cz-Si by deep-level transient spectroscopy (DLTS) and found two activation energies for electron emission corresponding to a shallow (1.01 ± 0.1 eV) and a deeper level (0.91 ± 0.1 eV). These were, however, considered not to be effective as recombination centers.[12]

Imaging of the spatial distribution of TDs in Cz-Si has previously been performed by others. Hu et al. used carrier density imaging (CDI) to map TDs in vertically cut mirror-polished slabs of n-type material. Niewelt et al.[13] did conventional nonspectrally resolved PL imaging of as-cut p-type wafers before and after the formation of TD. In both these works, the images were combined with resistivity measurements to obtain a concentration map of O_i.

Our group represented by Mehl et al. was the first to use and report on hyperspectral PL-imaging methods on Cz-silicon wafers.[14] This work showed that the DRL signal of 0.767 eV was distributed in a ring-like pattern and that regions showing high intensities of the P-line signal could be connected to interstitial oxygen.

In the current work, hyperspectral PL imaging has been conducted on Cz-silicon wafers that have been exposed to heat treatments at 450 and 650 °C with the purpose of studying the spatial distribution of the PL signals related to TDs. The treatments were performed on samples with both high and low interstitial oxygen concentration to compare them. It was expected from the literature referenced previously that the generation rate of TDs would be higher in oxygen-rich material.

2. Experimental Section

The samples used in this study were taken from commercially produced n-type Cz-silicon ingots of high quality. Samples were selected as two sets of five sequential wafers from the seed- (S) and tail (T) end of two different ingots. The wafers measured 125×125 mm^2 with a wafer thickness of 125 μm. The sample details as given by the manufacturer are shown in **Table 1**. The samples were received as-cut and were kept as-cut during the study.

The thermal annealing of the samples was performed in a quartz tube furnace (Tempress). The sample compartment was flushed by N_2 (AGA grade 5.0, 99.999%) to reduce oxidation. The wafers were placed on a quartz stand and had no physical contact with any other surface under the annealing process. Before heat treatment, the samples were cleaned by an HF dip for 2 min. A deep rinse was then performed by 8 min immersion in Piranha solution ($H_2SO_4 + HF$) with a last HF dip for 2 min. After each treatment, the samples were rinsed with deionized (DI) water and dried in N_2. The samples were then heat treated for 24, 66, and 99 h at 450 °C, respectively. The samples

ADVANCED
SCIENCE NEWS
www.advancedsciencenews.com

physica
status
solidi a

www.pss-a.com

Table 1. Sample properties as given by the manufacturer.

Sample set	Samples	O_i [ppma]	C_s [ppma]	R [Ω cm]	Ingot
S2	1–5	17.23	0.07	11.8	1
T2	1–5	8.37	2.68	2.2	2

Table 2. Treatment details for the samples used in this study.

Sample set	Sample	450 °C	650 °C
S2	S2-1		
	S2-2-24	24 h	
	S2-3-66	66 h	
	S2-4-650	24 h	1 h
	S2-5-99	99 h	
T2	T2-1		
	T2-2-24	24 h	
	T2-3-66	66 h	
	T2-4-650	24 h	1 h
	T2-5-99	99 h	

Table 3. Overview of the PL emissions discussed in this study.

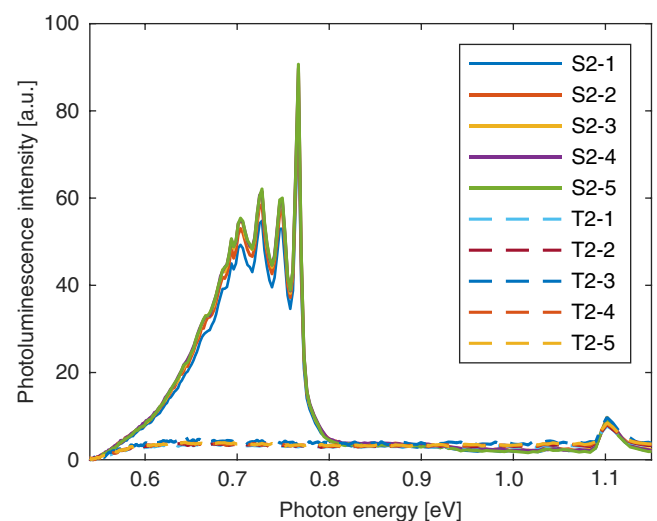| Emission	Peak energy [eV]	Comment
P-line	0.767	[6,17]
P067	0.666	
P069	0.693	
P070	0.702	
P072	0.724	
P074	0.746	
H	0.925	With P-line
BB	1.10	Band-to-band
D1	0.807	Much studied

Figure 1. Spectral PL response upon excitation for the untreated wafer sets. The BB transition at 1.1 eV is recorded with similar strength for all the wafers. The seed-end wafers (S2-1–S2-5) all exhibit strong DRL in the band 0.6–0.8 eV which is absent in the tail-end samples.

annealed at 650 °C were first treated at 450 °C for 24 h. After each treatment, the samples were rapidly cooled in N_2 at room temperature. The sample names and their individual treatment details are shown in **Table 2**.

Spectrally resolved PL images of the samples were recorded by hyperspectral imaging with a near-infrared (NIR) pushbroom camera (Specim, SWIR) equipped with a HgCdTe detector with sensitivity in the range of 0.49–1.33 eV, spectral resolution of 6 nm. The spatial resolution was 500 μm for this setup. The excitation source was a 808 nm line laser (Coherent, Lasiris Magnum II) with a radiated power density of 1.8 Ω cm^{-2}. The samples were positioned on a liquid N_2-cooled sample holder with a polished aluminum surface cooled at 85–90 K. The average photon penetration depth in silicon for radiation at 808 nm at this temperature is 65 μm. The specific details regarding the technique used has been thoroughly described in previously published articles.[14–16]

3. Results and Discussion

In this section, the results will be presented as an integrated spectrum over the whole wafer for the seed- and tail-end samples, respectively. Spatially resolved images of different PL emissions from the wafers with artificial colors will be presented along with the spectrum with discussion of the results. **Table 3** shows both previously reported emission lines relevant here and new signals reported in this study.

3.1. Spectral PL Response and Images of Untreated As-Cut Wafers

Figure 1 shows the mean spectra of the sample sets. Multiple emission lines can be observed within the spectral range

of 0.666–0.767 eV. The peaks are located at 0.767, 0.746, 0.724, 0.703, 0.693 eV, and with a distinct shoulder at 0.666 eV. The DRL appears strong in the seed-end wafers and not present in the tail-end samples.

The emission lines found in the out-of-the-box samples have been marked from 1 to 7 in **Figure 2**, where 1–6 are powerful DRL emissions in the range of 0.666–0.767 eV. The emission lines are listed with assigned names starting with P as they all seem related to the primary P-line. P067 at 0.666 eV, P069 at 0.698, P070 at 0.703 eV, P072 at 0.724 eV, and P074 at 0.746 eV with similar spatially distribution. The signal at 0.767 eV has been denoted as the primary P-line as described in previous studies.[6,14]

The samples within the same set show a high degree of similarity in the spectral and spatial distribution of the DRL signals. The seed-end wafers with a higher O_i content exhibit strong DRL emissions with similar strength, whereas the tail-end wafers being low in O_i do not exhibit them. As mentioned previously, the emission at 0.767 has been denoted as the P-line
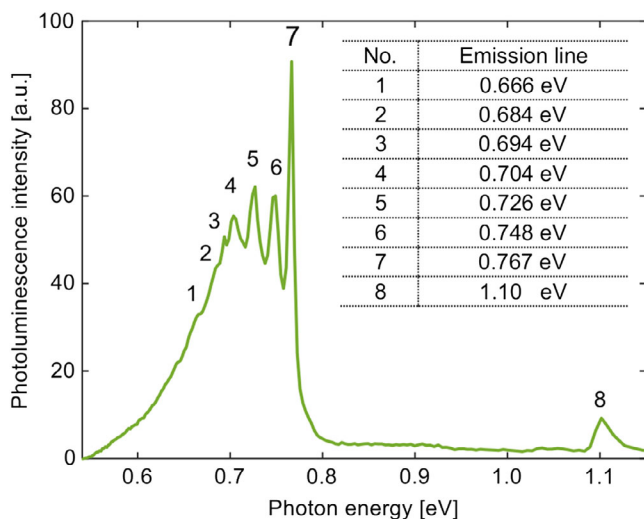
Figure 2. Nomenclature used for the P-line-related DRL- and the direct BB emissions.

in earlier studies and has been connected to TDs as it was first described in thermally annealed samples with high oxygen content. The seed-end part of the ingot is generally considered to contain higher concentrations of TDs.

The sharp peaks at P067, P069, P070, P072, and P074 have previously been described by Mehl et al.[14] There, it was concluded that the emission lines (and the primary P-line) were due to TDs and that the defects were spatially distributed in a ring-like pattern. The current results support this.

In addition to the DRL signals, the direct band-to-band (BB) signal can be observed in the spectra at 1.1 eV. The intensity of the BB signal is very low, which can be expected in as-cut samples, as this is an effect of a high level of surface recombination having a pronounced effect on the slow, direct BB transition requiring phonon interaction. Recombination through the direct BB mechanism is in general supposed to be substantially slower than recombination through traps in the bandgap through the Shockley–Read–Hall (SRH) mechanism. The emissions seen in the energy range of 0.666–0.767 eV are likely due to recombination at traps placed near midgap and are therefore considered as deep-level traps. These are known to be very effective
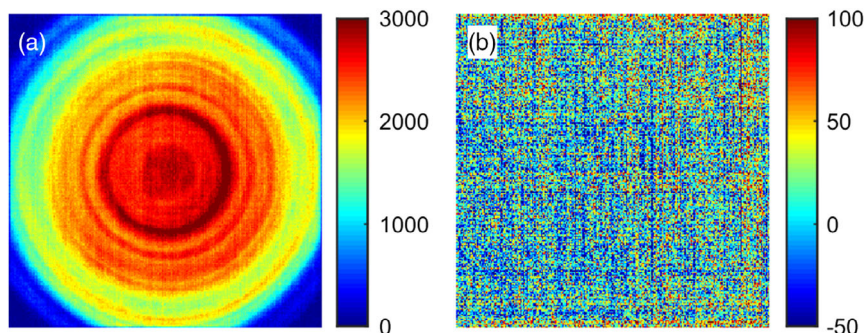
recombination centers and may explain the high DRL signals. Furthermore, the recombination rate through traps is directly proportional to the number of empty traps and the concentration of electrons in the conduction band. The defects responsible for the P-line-related DRL pattern must therefore be present in high densities to cause the intense emissions seen in the mean spectra.

Figure 3 shows the spatial distribution of the DRL signals in the untreated wafers a) S2-1 (seed) and b) T2-1 (tail). The images were created by integrating the luminescence signal over the wavelength range of 0.666–0.767 eV. The general characteristic of the spatial distribution of the signal is that it accumulates in a ring-like pattern and radially increases toward the center of the wafer. The signal is absent at the edges and not present in the tail-end sample T2-1.

3.2. Spectral PL Response and Images of Thermally Annealed Seed-End Wafers

The mean spectra of the thermally annealed seed-end samples are shown in **Figure 4**. The samples were heated and cooled once. The exception is the S2-4-650 sample which received a two-step
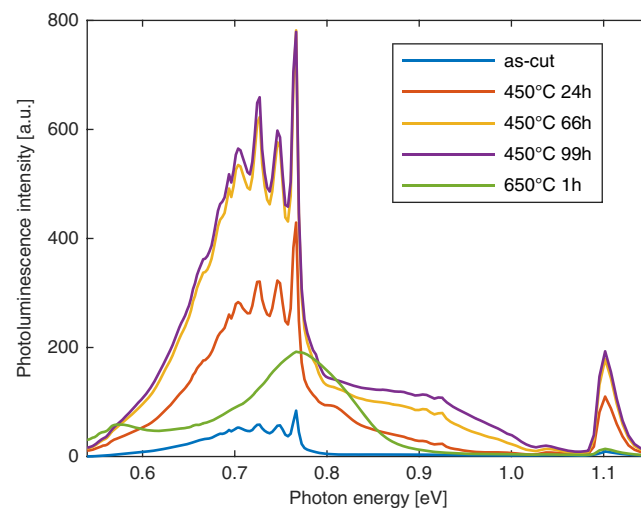

Figure 4. Spectral PL response from the seed-end wafers before and after thermal treatments.

Figure 3. Image of the defect-related (0.666–0.767 eV) emissions in a) a seed-end wafer and b) a tail-end wafer. The samples were out-of-the-box as-cut and untreated.

annealing as shown in Table 2. The spectra for the samples treated at 450 °C show substantial growth of the peaks between 0.666 and 0.767 eV as a result of the heat treatment. The peak at the primary P-line (0.767 eV) is the most prominent. Careful examination of the individual strength of the peaks reveals that their relative development differs over time. Relative to strength of the primary P-line (0.767 eV), the emission strength of the line at 0.748 eV (no. 6) is rising only to a little extent compared with the primary P-line after 24 h of heat treatment. The others (no. 1–5) are still rising substantially both in relative and absolute strength after 99 h. This suggests that they stem from different TD complexes. No spatial differences have been found, but as the samples investigated in this study are as-cut with substantial surface scattering, this may not be the case on polished samples. The individual temporal and spatial development of the peaks in the P-line complex calls for more in-depth investigations in dedicated studies. The annealing process also introduced several new emission lines into the mean spectra, at 0.807, 0.904, and 0.925 eV. Two of the signals have been named in existing literature, where the signal at 0.807 eV is referred to as the D1 signal and the weak signal at 0.925 eV is referred to as the H-line.[6] A weak emission at 0.903 eV has previously been studied by us and is referred to as D090.[16] This coincides with the deeper level recently reported by Markevich et al.[12] Further referring to this work, a shoulder at 1.01 eV associable with the corresponding shallow level is barely visible. The weak nature of these emissions in our data supports the conclusion that these are not effective recombination centers. The growth of the DRL signals continue up to somewhere between 66 and 99 h of annealing, as it is evident that the height of the peaks are almost identical in S2-3-66 and S2-5-99. Only small changes can be seen in the growth of the intensity between the D090 and the H-line signals. The direct-transition BB luminescence signal is affected by the annealing and show a marked increase. However, the intensity of the BB signal never exceeds the intensities of observed emission lines between 0.666 and 0.767 eV.

After annealing at 650 °C, the mean spectra of sample S2-4-650 show a complete spectral redistribution of the DRL. This eliminated the peaks at P069, P070, P072, P074, D090, and the H-line.[6,16,18] Instead, a wide emission band has formed between 0.66 and 0.85 eV with a peak at the P-line. The BB signals have been reduced to intensities, which was seen in the as-cut samples, prior to any of the process steps.

The previously reported D1 (0.807 eV), H (0.925 eV), and D090 (0.900 eV) emissions are not found in the spectra from the untreated samples (Figure 1).[6,16,18] The heat treatment at 450 °C has a marked effect on these as they emerge and get stronger with heat treatment as does the P-line complex. The H-line is reported to appear together with the P-line, whereas the D090 signal is reported to be present in multicrystalline material.[16] The D1 signal is reported in multicrystalline material and in intentionally deformed Cz wafers with high content of extended dislocations.[18] The 650 °C anneal effectively removes both the H and D090 emissions, whereas the shape of the broadband emission experienced after 650 °C might be a superposition of a strong signal with center energy of 0.767 eV and the D1 signal as it exhibits a shoulder at higher energies. Multivariate curve resolution (MCR)—a statistical method for

deconvolving complex signals—which is extensively reported on elsewhere[14,16,19,20] partitioned the broad emission into two separate signals, one of them is the D1 emission. The D1 signal is commonly considered to be caused by recombination through states in the band gap introduced by dislocations or impurities decorating these.

The spatial distribution and strength of the defect-related emission due to recombination via the SRH mechanism in the range of 0.666–0.767 eV (Figure 4) for the seed-end wafers as function of treatment are shown in **Figure 5**. It is evident that the strength of the DRL increases drastically upon treatment at 450 °C. A ring-like structure is kept during the treatments, albeit slightly less pronounced for the longer treatments. The signal expands systematically with treatment time from primarily being present in the ingot center in the untreated wafers (Figure 5a) to cover most of the wafer except near the edges after 99 h (Figure 5d).

The 1 h annealed at 650 °C after 24 h at 450 °C for the sample in Figure 5e completely removes the ring structure and the whole sample seemingly responds homogenously to the excitation for the defect-related signals.

The spatial distribution and strength for the PL due to the direct Si BB transition in the range of 1.098–1.114 eV in the samples are shown in **Figure 6**. The untreated sample shows very little PL in this range. This probably reflects very high surface recombination in the as-cut samples.

A remarkable feature is that the development of the defect-related signals after heat treatment at 450°C in a way activates the material to respond more intensely on excitation also for the BB transition. BB recombination emitting at 1.10 eV necessarily involves phonon interaction (Si being an indirect bandgap material at this excitation wavelength), so this mechanism is associated with a substantially long diffusion length of the charge carriers before recombination occurs—in particular in cooled samples like these. This enables the surface recombination to have a much stronger influence on the BB signal than on the DRL-related emissions from rapid recombination through traps in the bandgap not necessarily involving phonons. Increased BB recombination over the bandgap points to a large increase in the injection level of free charge carriers. If the P-line-connected emissions in the range of 0.666–0.767 eV are due to recombination through deep-level traps introduced by TDs, one would expect the opposite—a lower injection level. In Figure 4, it is evident that the BB signal develops along with the DRL signal upon heat treatment at 450 °C. The 1 h anneal at 650 °C seems to effectively kill the BB luminescence which is developed at the lower temperature. This is a strong indication that the broadband emission with center energy of 0.767 eV experienced after annealing at 650 °C has a different origin than the sharp and similarly intense energetic P-complex photons.

3.3. Spectral PL Response and Images of Thermally Annealed Tail-End Wafers

The mean spectra from the tail-end samples are shown in **Figure 7**. Note that the 24 h sample (T2-2-24) cracked diagonally during handling. The image of the top right half sample is shown in Figure 7a. The untreated sample did not exhibit any DRL and
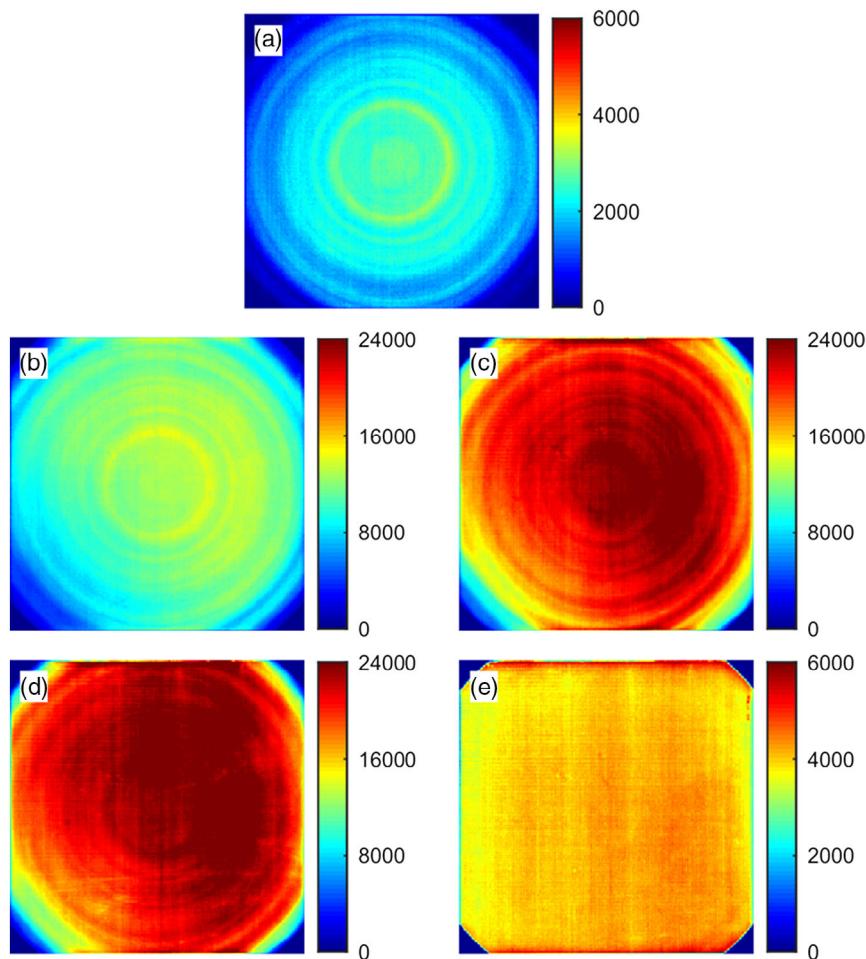
ADVANCED
SCIENCE NEWS
www.advancedsciencenews.com

pss a
physica status solidi
www.pss-a.com

Figure 5. Images of PL due to recombination via the SRH mechanism for the defect-related part of the spectrum (Figure 4: 0.666–0.767 eV) in the seed-end wafers: a) untreated, b) 450 °C/24 h, c) 450 °C/66 h, d) 450 °C/99 h, and e) 450 °C/24 h + 650 °C/1 h.

the BB luminescence was found at a low level similar with all the other wafers as out-of-the-box. Upon heat treatment, a similar pattern as with the seed-end wafers appeared; a characteristic complex of at least six PL signals in the band 0.666–0.767 eV grew steadily upon prolonged heat treatment at 450 °C. A 1 h treatment at 650 °C after 24 h at 450 °C produced a strong, broad-band emission with center energy around the primary P-line (0.767 eV).

There are, however, a few notable differences. First, the strength of the emissions is substantially lower than for the seed-end wafers. Second, the BB signal did not completely disappear after treatment at 650 °C, although anneal at this temperature diminished it. Third, strong additional signals appeared. Most notable is the previously described D1 signal frequently ascribed to impurities (most studies mention Fe) interacting with dislocations. The results reported here supports the theory that the D1 signal is related to impurities such as Fe as the tail end of the Cz ingot is supposed to contain small, but substantially larger amounts of metallic impurities than the seed end. This is due to the refining effect while pulling the solid ingot from molten Si. Silicon exhibits distribution coefficients between solid/molten materials for metallic impurities in the 10^{-3}–10^{-8}

range. Metallic impurities will build up in the molten metal and substantially increase in the ingot tail. However, as noted previously, these wafers do not exhibit extended dislocation networks, strongly indicating that the D1 emission is not dependant on such to be present. However, our results support the notion that the D1 signal is related to oxygen: clusters or precipitates. The D1 signal is not found in the untreated tail-end wafers and only appear together with the emergence of the P-line complex (0.666–0.767 eV). As this is ascribed to TDs caused by oxygen clusters forming, finding the D1 signal only when these have appeared is a strong indication for this.

The spatial distribution and strength of the defect-related signal in the band 0.666–0.767 (the P-line complex) as function of heat treatment are shown in **Figure 8**. As for the seed-end wafers, the signal is distributed in a ring-like pattern when subject to treatment at 450 °C. Treatment at 650 °C destroys the ring-like pattern and the broad signal appearing is more or less evenly distributed.

Images of the distribution of the D1 signal in tail-end wafers are shown in **Figure 9**. Heat treatment at 450 °C brings out a weak ring-shaped pattern, whereas subsequent treatment at 650 °C makes for an evenly, more homogenous distribution.
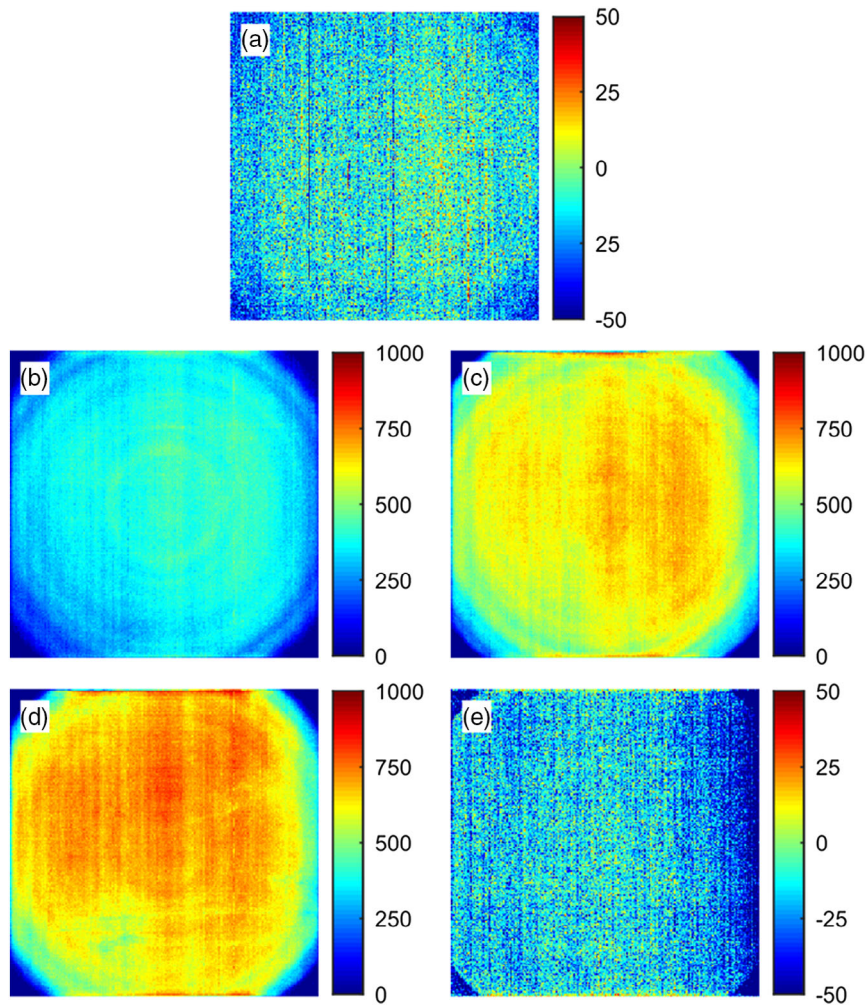
1900884 (6 of 9)

Figure 6. Images of PL due to recombination via the direct BB mechanism (Figure 4: 1.089–1.114 eV) in the seed-end wafers: a) untreated, b) 450 °C/24 h, c) 450 °C/66 h, d) 450 °C/99 h, and e) 450 °C/24 h + 650 °C/1 h.
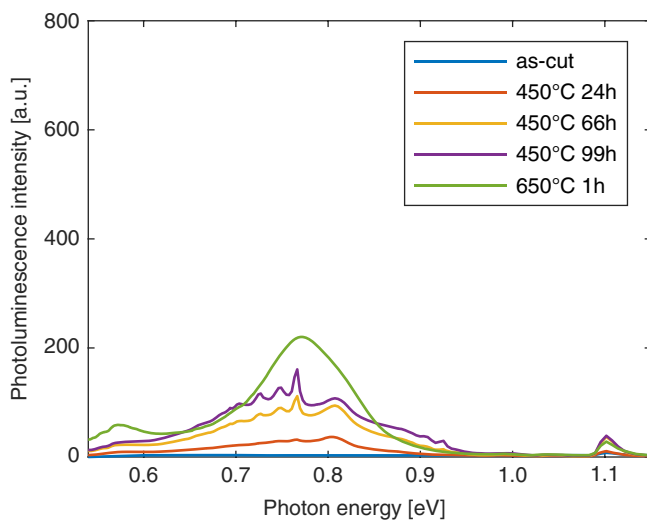

Figure 7. Spectral PL response from the tail-end wafers before and after thermal treatments.

The results support the generally accepted mechanisms for TD formation. Untreated out-of-the box seed-end samples have experienced temperatures of around 450 °C during crystal pulling. They also contain a certain amount of oxygen. Interstitial oxygen is routinely measured in thicker wafers—or "slugs," by the manufacturer by Fourier-transform infrared spectroscopy (FTIR)—capable of detecting O_i but not clusters and precipitates. Our seed-end samples contained 17.23 ppma O_i, and a certain amount of TD had formed during manufacture as shown in Figure 4 ("as-cut"). The P-line has been securely tied to TDs which again is commonly believed to be caused by small oxygen clusters containing a handful of atoms. There are reportedly only a limited number of types of such characteristic clusters.[4] Our spectra (Figure 2 and 4) indicate seven such characteristic clusters to be present in the seed-end wafers after heat treatment at 450 °C for 99 h. The multiplication of TDs leads to an increased injection level of free charge carriers in the conduction band upon excitation. This leads to increased signal also from the direct BB recombination mechanism. At 650 °C, the diffusion of oxygen is enhanced in the silicon bulk structure and the small,
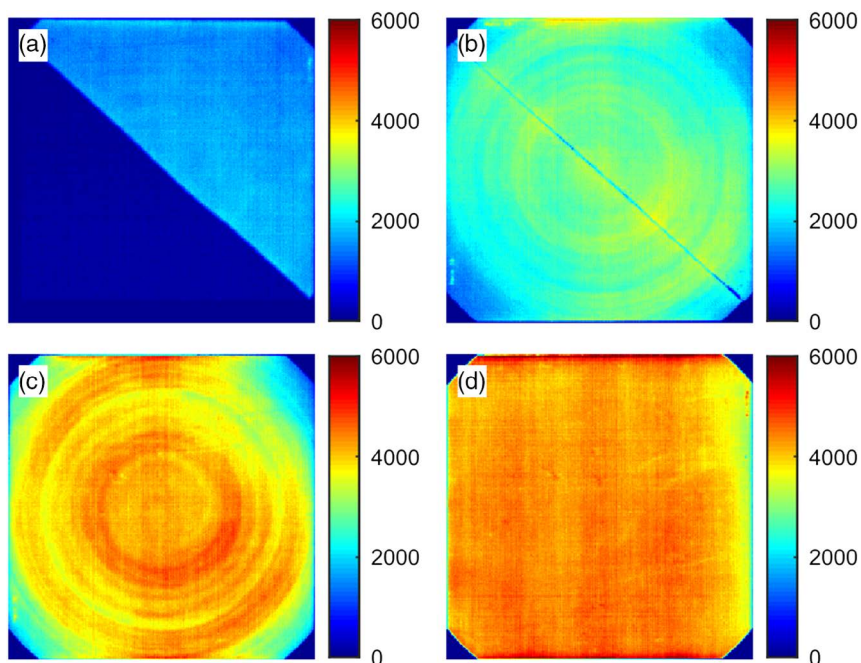
Figure 8. Images of PL due to recombination via the SRH mechanism for the P-complex-related part of the spectrum (Figure 7: 0.666–0.767 eV) in the tail-end wafers: a) 450 °C/24 h, b) 450 °C/66 h, c) 450 °C/99 h, and d) 450 °C/24 h + 650 °C/1 h. No signal was recorded in the untreated sample. The sample in part (a) accidentally broke during handling.
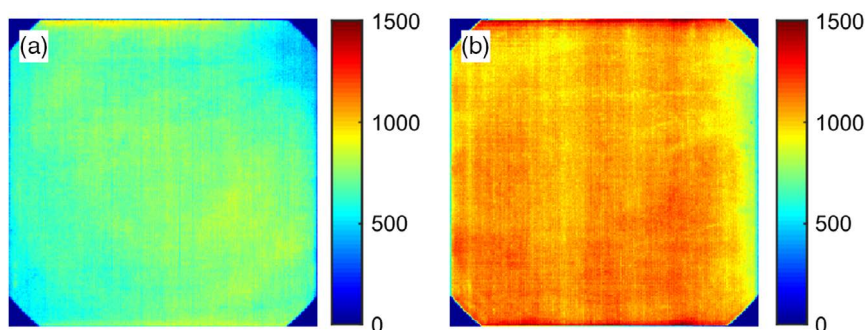

Figure 9. Image of the distribution of the D1 signal (0.804–0.810 eV) in tail-end wafers: a) after 99 h treatment at 450 °C and b) after 450 °C/24 h + 650 °C/1 h.

TD-forming clusters disappear while larger precipitates form. These are more recombinant active, remove the donor states, and effectively quench the signal from the BB transition. The enhanced diffusion leads to loss of the ring-like structure.

The tail-end wafers had not experienced prolonged temperatures in the 450 °C range during the manufacturing process. As-received, they did not exhibit any DRL emissions attributable to TDs. Upon heat treatment at 450 °C, the characteristic seven-emission P-complex linked to TDs formed, systematically growing with time. The content of O_i was about half of that in the seed-end material (8.37 ppma) leading to a substantially lower number of TD clusters forming in the tail-end wafers. Treatment at 450 °C enhanced the emission from the BB mechanism, also for the tail-end wafers. Heat treatment at 650 °C again removed the characteristic, ring-like P-complex and a

similar broadband emission with center energy 0.767 eV formed as seen for the seed-end wafers. Again, the BB signal became weaker, albeit not to the same extent as for the seed-end wafers. The behavior of the BB signal is difficult to explain and should be the subject for further studies.

4. Conclusions

In this study, we report on the combination of spectroscopy and imaging on heat-treated Cz-Si wafers made possible by hyperspectral imaging methods. The primary objective has been to study defect-related PL in the material as function of position in the ingot and the application of different thermal treatments. The seed-end wafers exhibited a complex range of emissions due

to defects associated with the P-line emission at 0.776 eV without any heat treatment. This indicates that the wafers contained TD oxygen clusters after manufacture. These were distributed in a ring-like pattern in the wafers. The tail-end wafers did not exhibit this. Heat treatment at 450 °C strongly enhanced the signal strength from the P-complex of signals both in the seed- and the tail-end wafers. Other DRL-related signals also appeared upon treatment at 450 °C, particularly can be noted the D1 signal emerging in the tail-end wafers after 24 h. The treatment at 450 °C systematically enhanced the signal from direct BB recombination. Treatment at 650 °C made for a redistribution of the signals having emerged at the lower temperature. The strong P-line complex of signals with six sharp emission lines disappeared, and a broad signal with center energy approximately the same as the primary P-line at 0.767 eV appeared. Treatment at this temperature made the BB signal disappear in the seed-end wafers and to diminish in the tail-end wafers. The results support the general consensus for TD formation. In further studies, the combination of spectral PL should be complemented with other methods such as resistivity mapping, electroluminescence (EL), and light-beam-induced current (LBIC). Such studies could provide new insight into the mechanisms behind TDs.

Conflict of Interest

The authors declare no conflict of interest.

[1] C. S. Fuller, R. A. Logan, *J. Appl. Phys.* **1957**, *38*, 1427.
[2] W. Kaiser, H. L. Frisch, H. Reiss, *Phys. Rev.* **1958**, *112*, 9.
[3] M. Tajima, P. Stallhofer, D. Huber, *Jpn. J. Appl. Phys. Part 1* **1983**, *22*, L586.
[4] D. K. Schroder, *J. Appl. Phys.* **1988**, *63*, 7.
[5] U. Gösele, T. Y. Tan, *Appl. Phys. A: Mater. Sci. Process.* **1982**, *28*, 14.
[6] N. S. Minaev, A. V. Mudryi, *Phys. Status Solidi A* **1981**, *68*, 5.
[7] P. Wagner, J. Hage, *Appl. Phys. A: Mater. Sci. Process.* **1989**, *49*, 123.
[8] R. C. Newman, *J. Phys.: Condens. Matter* **2000**, *12*, R335.
[9] V. V. Voronkov, *J. Electrochem. Soc.* **2000**, *147*, 8.
[10] W. Götz, *J. Appl. Phys.* **1998**, *84*, 8.
[11] K. Kinoshita, T. Kojima, K. Onishi, Y. Ohshita, A. Ogura, *Jpn. J. Appl. Phys.* **2019**, *58*, 6.
[12] V. P. Markevich, M. Vaqueiro-Contreras, S. B. Lastovskii, L. I. Murin, M. P. Halsall, A. R. Peaker, *J. Appl. Phys.* **2018**, *124*, 6.
[13] T. Niewelt, S. Lim, J. Holtkamp, J. Schon, W. Warta, D. Macdonald, M. C. Schubert, *Sol. Energy Mater. Sol. Cells* **2014**, *131*, 117.
[14] T. Mehl, I. Burud, E. Letty, E. Olsen, *Energy Procedia* **2017**, *124*, 6.
[15] E. Olsen, A. S. Flo, *Appl. Phys. Lett.* **2011**, *99*, 011903.
[16] E. Olsen, S. Bergan, T. Mehl, I. Burud, K. E. Ekstrøm, M. DiSabatino, *Phys. Status Solidi A* **2017**, *214*, 8.
[17] M. Tajima, Y. Iwata, F. Okayama, H. Toyota, H. Onodera, T. Sekiguchi, *J. Appl. Phys.* **2012**, *111*, 113523.
[18] N. A. Drozdov, A. A. Patrin, V. D. Tkachev, *JETP Lett.* **1976**, *23*, 597.
[19] I. Burud, T. Mehl, A. S. Flø, D. Lausch, E. Olsen, *J. Spectral Imaging* **2016**, *5*, a8.
[20] D. Lausch, T. Mehl, K. Petter, A. S. Flo, I. Burud, E. Olsen, *J. Appl. Phys.* **2016**, *119*, 054501.